Chapter 20
Mechanical Behavior of Cast Plastic-Bonded Explosives

Hai Nan, Chunyan Chen, Yufan Bu, Yulei Niu, and Xuanjun Wang

Abstract Influential factors on the mechanical behavior of cast plastic-bonded explosives (PBXs) were investigated through compression tests in this paper. Different mechanical behaviors of PBXs were observed when PBXs were prepared with different curing temperatures, different molecular weights and different NCO/OH values of hydroxyl-terminated polybutadiene (HTPB). Based on stress–strain curves of PBXs, mechanical behavior is divided into brittle fracture and ductile fracture. The results show that PBX ranges from ductile fracture to brittle fracture when the curing temperature increases from 50 to 100 °C, molecular weights decrease from 4000 to 1500 and NCO/OH value increases from 0.8 to 1.4. Besides, the microstructure of PBXs was characterized with scanning electron microscopy (SEM), indicating that energetic particles were damaged by the brittle fracture.

20.1 Introduction

With the rapid development of energetic materials, cast plastic bonded explosives (PBXs) have attracted tremendous attention because of their good dimensional and thermal stability, and low vulnerability. But the sensitivity of PBX, in which micron-sized explosive crystals are embedded in a polymer binder matrix, is enhanced due to the cracks in the energetic crystals [1, 2], which may also generate "hot spots" in PBX loads [3]. To avoid these cracks by enhancing the mechanical properties of PBX, various methods have been developed, including introducing bonding agent to PBX and adjusting the crosslinking network of the polymer matrix [4–7].

The cracks in the energetic crystals are related to not only the mechanical property of PBX but also the mechanical behavior [8–10]. Palmer and Thompson [11, 12] demonstrated that through a quasi-static test, PBX was extensively deformed,

H. Nan · X. Wang (✉)
High-Tech Institute of Xi'an, Xi'an 710025, P.R. China
e-mail: wangxj503@sina.com

H. Nan · C. Chen · Y. Bu · Y. Niu
Xi'an Modern Chemistry Research Institute, Xi'an 710065, P.R. China

A. Gany and X. Fu (eds.), *2021 International Conference on Development and Application of Carbon Nanomaterials in Energetic Materials*, Springer Proceedings in Physics 276,
https://doi.org/10.1007/978-981-19-1774-5_20

and thus the distortion and damage of the energetic particles were avoided, and the generation of PBX "hot spots" was restrained. Thus far, the changeable mechanical behavior of thermosetting hydroxyl-terminated polybutadiene (HTPB)-based cast PBX has been investigated. The results of quasi-static and dynamic compression tests on PBX showed that the mechanical behavior of PBX is strongly influenced by strain rate and temperature [13–16]. However, the factors that influence the mechanical behavior of the thermosetting PBX have not been examined. Therefore, the effects of curing temperature, molecular weights and NCO/OH value of HTPB on the mechanical behavior of PBX were investigated in this paper. The findings are significant for the mechanical behavior control and safety of PBX.

20.2 Experiment

20.2.1 Materials

HTPB was utilized as the binder in PBX. The considered molecular weights of HTPB were 1500, 2800, 3440, and 4000, and the corresponding hydroxyl values were 1.55, 0.78, 0.61, and 0.59 mmol g^{-1}, respectively. Samples were obtained from Liming Chemical Research Institute and were pre-degassed for 4 h at 80 °C. 2,4-toluene diisocyanate (TDI) was purchased from Beijing Chemical Reagent Company and used as the curing agent. TDI was pre-redistilled before use. Dioctyl adipate (DOA) was employed as the plasticizer. Aluminum (Al) and 1,3,5-trinitroperhydro-1,3,5-triazine (research department explosive (RDX)) were utilized as energetic particles.

20.2.2 Preparation of Elastomeric Films

HTPB and TDI were stirred for 10 min at 60 °C in a vertical kneading machine (2 L) to generate a liquid–liquid mixture. Triphenyl bismuth (TPB, 0.01%) was then added to the liquid–liquid mixture and stirred for 30 min at 60 °C to produce thermosetting HTPB slurry. The slurry was then poured into a Teflon mold (12 mm × 10 mm × 2 mm) to fabricate elastomeric films. The films were cured at 60 °C until the hardness stabilized. Finally, the films were removed from the Teflon mold.

20.2.3 Preparation of Cast PBX

HTPB and DOA were stirred for 10 min at 60 °C in a vertical kneading machine (2 L) to generate a liquid–liquid mixture. Al and RDX were then added to this mixture and stirred for 1 h at 60 °C to produce a solid–liquid mixture. TPB and TDI were added

Table 20.1 Composition of HTPB-based PBX

Sample	Composition
PBX1(HTPB1500)	RDX/Al/HTPB/DOA/TDI/TPB (64.00/20.00/6.99/8.00/1.01/0.01)
PBX2(HTPB2800)	RDX/Al/HTPB/DOA/TDI/TPB (64.00/20.00/7.45/8.00/0.55/0.01)
PBX3(HTPB3440)	RDX/Al/HTPB/DOA/TDI/TPB (64.00/20.00/7.56/8.00/0.44/0.01)
PBX4(HTPB4000)	RDX/Al/HTPB/DOA/TDI/TPB (64.00/20.00/7.57/8.00/0.43/0.01)

to the solid–liquid mixture and stirred for 20 min at 60 °C to obtain the PBX slurry. The PBX slurry was then poured into the mold (Φ20 mm × 20 mm) and cured at 60 °C until the elastic modulus of PBX was constant. The PBX was then removed from the stainless steel mold. Table 20.1 shows the details of the formulation of the HTPB-based PBX.

20.2.4 Characterization

The dumbbell-shaped elastomer underwent tensile tests with an Instron Universal Testing Machine (Model 4505) at a crosshead speed of 500 mm/min. The tests followed the GJB770B-2005 test method, and the final test values were derived from an average of at least five specimens at 25 °C.

The compression tests on PBX followed the GJB 772A-97 test method under the following conditions: a temperature of 25 °C and a crosshead speed of 10 mm min^{-1}. The samples were cut in the dimensions of 20 mm × 20 mm × 3 mm.

The elastic modulus was calculated based on the compression stress–strain curves when the strain was 0.3%, and the elastic modulus was calculated using Eq. 20.1 as follows:

$$E = \sigma/\varepsilon \tag{20.1}$$

where E is the elastic modulus, and σ and ε are stress and strain, respectively.

Crosslink density was calculated based on the swelling parameters of the networks [16]. The elastomers that measured 7 mm × 7 mm × 3 mm were placed in toluene for 48 h. They were then removed from the solvent and weighed after the solvent was wiped from the elastomer surface. Subsequently, the solvent absorbed by the elastomer was released by placing the swollen elastomer in a vacuum oven at 110 °C for 3 h. The weight of the deflated elastomer was then determined. The volume fraction of the elastomer in the swollen specimen (V_1) was calculated based on the weights of the swollen and deflated specimens and the densities of the elastomers. The crosslink density of the elastomer (V_e) was obtained from using Eq. 20.2:

$$V_e = -\left[\ln(1 - V_1) + V_1 + \chi V_1^2\right] / V_s\left(V_1^{1/3} - V_1/2\right) \tag{20.2}$$

where V_s is the molar volume of the solvent and χ is the elastomer-solvent interaction parameter.

The microstructure of the compressed PBX was examined through a scanning electron microscope (SEM).

20.3 Results and Discussion

20.3.1 Mechanical Behavior of the Cast PBX

Figure 20.1 shows the results of compression tests, respectively. The failure mechanisms were characterized by brittle and ductile fractures based on stress–strain curves of PBXs. When the PBXs display a brittle fracture, stresses are often linearly related to strain in the long term. Stress has a nonlinear relationship with strain only when the load approaches maximum stress. In the event of sudden brittle fracture, stress is rapidly maximized in mechanical tests. The stress in ductile fracture is linearly related to strain in the short term and is nonlinearly associated with strain over the long term. Following crack formation, strain increases and the crack can widen gradually over a period of time. Severe deformation causes the PBX to resemble a "drum". Moreover, fractures are typically initiated at its center.

To further investigate the fracture mechanism of PBX, the RDX, post-loaded RDX and microstructure of the post-compression PBX were characterized with SEM, as indicated in Figs. 20.2a, b and 20.3, respectively. The crack can evidently be observed on the post-loaded RDX. However, no crack arises in PBXs with ductile fractures, this finding can be attributed to PBXs ductile deformation, which mainly originates from binder strain after PBXs are loaded. The severe deformation of the binder effectively protects the energetic particles from damage in the event of ductile fracture. On the contrary, the brittle fracture with small deformation generates some cracks and damages energetic particles because stress concentration appears on the hard RDX.

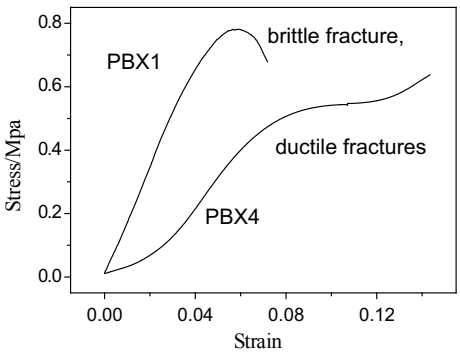

Fig. 20.1 Stress–strain curves of PBX4 in compression test

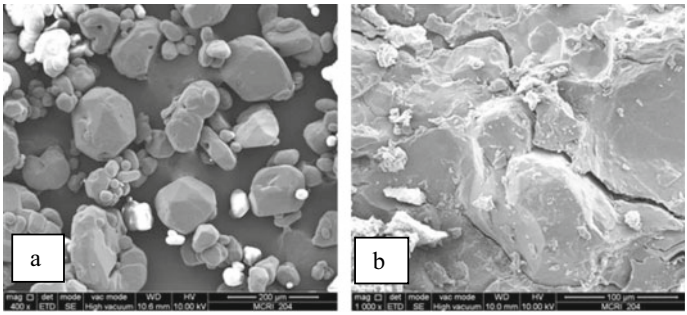

Fig. 20.2 SEM images of **a** RDX and **b** post-loaded RDX

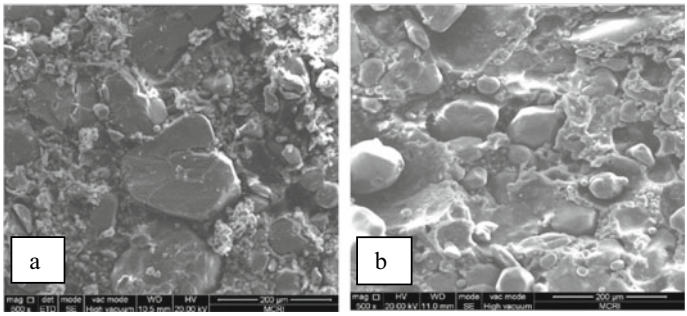

Fig. 20.3 **a** Brittle fracture and **b** ductile fracture of PBX

20.3.2 Effects of Curing Temperature on the Mechanical Behavior of Cast PBX

Curing temperature affects the mechanical behavior of PBX since a low curing temperature diminishes the elastic modulus and enhances compression strain. Figure 20.4 and Table 20.3 respectively depicts the compression curves and corresponding mechanical properties of PBX that were completely cured at different temperatures. The binder cured at 50 °C displays a large elongation at break and a low tensile strength, as shown in Table 20.2. The severe deformation in the binder absorbs the compression energy and plugs the crack in the PBX cured at 50 °C, which is in turn induced by compression stress. In the event of ductile fracture, the crack gradually widens but mends quickly, generating a platform in the stress–strain curve. The stress then increases with the strain, and the stress acting on the energetic particles is broken down by the deformation of the binder.

As indicated in Fig. 20.4, the increase in curing temperature induces an increase in the elastic modulus of PBXs and a decrease in its elongation at break. This result is attributed to the high crosslinking density of the binder and the high curing stress

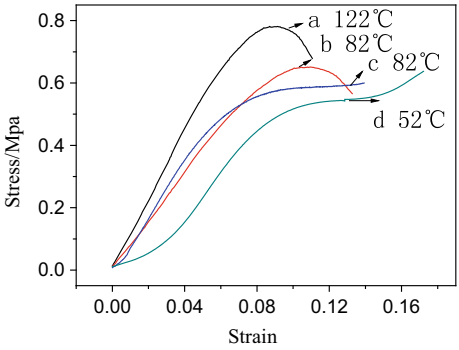

Fig. 20.4 The compression curves of PBX cured at different curing temperatures

Table 20.2 Mechanical properties of the elastomer at different curing temperature

Curing temperature (°C)	Tensile strength (MPa)	Elongation at break (%)	Crosslink density (mol/m^3)	Curing time (h)
50	1.01	181	80	144
60	1.17	128	85	123
70	1.19	112	97	90
80	1.23	101	102	75
100	1.26	95	107	50

Table 20.3 Crosslink density of the HTPB with different molecular weights

The binder	Crosslink density of the polymer (mol/m^3)
HTPB(1500)	112
HTPB(2800)	87
HTPB(3440)	81
HTPB(4000)	79

produced by increased curing velocity at high temperatures [17–19]. As a result, PBX experiences some brittle fractures.

The PBX thus displays ductile and brittle fracture behavior when the curing temperatures are 50 °C and 100 °C, respectively.

20.3.3 Effects of Molecular Weights on the Mechanical Behavior of Cast PBX

The cast PBXs that contains HTPB with different molecular weights were cured at 60 °C until the elastic modulus stabilized. The mechanical behavior of the PBXs

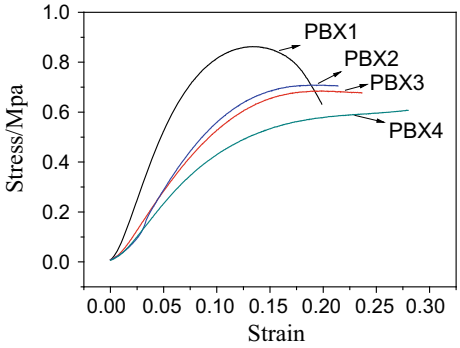

Fig. 20.5 Compression curves of PBX that contains HTPB at different molecular weights

was tested under a compression load, and the resultant test curves are presented in Fig. 20.5. When the molecular weights of the binder are low, PBX displays brittle fracture behavior and increased compression stress. The mechanical behavior of PBX transitions from brittle to ductile fracture with the increase in HTPB molecular weights, which is mainly attributed to the different crosslinking density, curing velocity and stress. Table 20.3 reveals that low molecular weight HTPB displays a high crosslinking density, moreover, excellent linear correlations are obtained between crosslink density and mechanical properties. The high crosslink density can increase stress and reduce elongation at break [7]. Meanwhile, curing velocity and stress of low molecular weight HTPB are higher than those of high molecular weight HTPB [18–20], which also renders the PBX brittle.

20.3.4 Effects of NCO/OH Value on the Mechanical Behavior of Cast PBX

With NCO/OH value ranging from 0.8 to 1.4, the mechanical behaviors of PBX change (Figs. 20.6 and 20.7). Compression strength increases and elongation at break

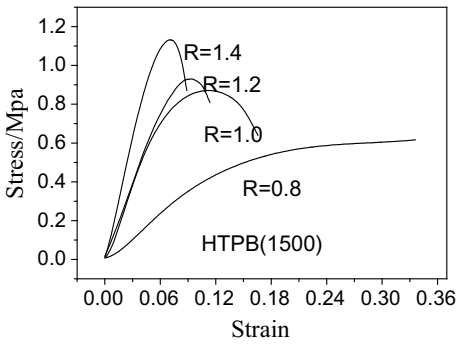

Fig. 20.6 The compression stress–strain curves of PBX including HTPB(1500) (R represents the NCO/OH value)

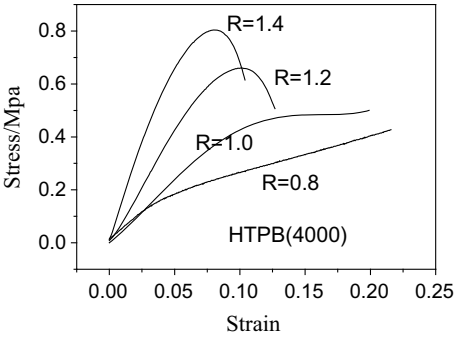

Fig. 20.7 The compression stress–strain curves of PBX including HTPB(4000) (R represents the NCO/OH value)

decreases with NCO/OH value. When NCO/OH value is 1.4 and 0.8, PBX obviously show brittle fractures and ductile fractures respectively. Effects of NCO/OH value on mechanical behavior are attributed to crosslink density of the binder, because the crosslink density of the polymer increases with NCO/OH value.

20.4 Conclusions

(1) The mechanical behavior of cast PBXs were investigated through compression tests. PBXs displayed two types of rupture behavior, namely, brittle and ductile fractures.
(2) The mechanical behavior of this cast PBX transitioned from ductile to brittle fracture, when curing temperature increased from 50 to 100 °C or NCO/OH value increased from 0.8 to 1.4. This result was attributed to the increase in crosslinking densities of HTPB.
(3) The mechanical behavior of PBX transitioned from brittle to ductile fracture as the molecular weights of HTPB increased from 1500 to 4000. This finding was attributed to the varied sizes of curing networks that led to the decrease of crosslinking densities and curing stresses.
(4) As observed in the SEM images of post-compression PBX, brittle fractures damaged energetic particles.

Acknowledgements The test support and useful discussion from Ms. Yang H. and Mr. Yang J. G. are greatly appreciated for our research.

References

1. C.B. Skidmore, D.S. Phillips, B.W. Asay, D.J. Idar, D.S. Bolme, Microstructural effects in PBX 9501 damaged by shear impact. Shock Compress. Condens. Matter 659–662 (1999)
2. V.D. Heijden, R.H.B. Bouma, Shock sensitivity of HMX/HTPB PBX's: relation with HMX crystal density, in *29th International Annual Conference of ICT*, Karsruhe, FGR, 30 June–3 July1998, pp. 65-1–65-11
3. J.E. Field, N.K. Bourne, S.J.P. Palmer, S.M. Walley, J. Sharma, B.C. Beard, Hot spot ignition mechanisms for explosives. Acc. Chem. Res. 489–496 (1992)
4. J.H. Liu, S.J. Liu, L.L. Chen, C.M. Lin, F.Y. Gong, F.D. Nie, Improving mechanical property of HMX-based PBX with neutral polymer bonding agent, in *Proceedings of the 45nd International Annual Conference of the Fraunhofer ICT*, Karlsruhe, Germany, 24–27 June 2014, pp. 56/1–56/8
5. F. Li, L. Ye, F. Nie, Y. Liu, Synthesis of boron containing coupling agents and its effect on the interfacial bonding of fluoropolymer/TATB composite. J. Appl. Polym. Sci. **105**, 777–782 (2007)
6. A. Balley, J.M. Bellerby, S.A. Kinloch, J. Shama, E.C. Baughan, M.M. Chaudhn, J.N. Sherwood, B.C. Beard, The identification of bonding agents for TATB/HTPB polymer bonded explosives. Philos. Trans. R. Soc. Lond. Ser. A **339**, 321–333 (1992)
7. J. Huang, L.N. Zhang, Effects of NCO/OH molar ratio on structure and properties of graft-interpenetrating polymer networks from polyurethane and nitrolignin. Polymer **43**, 2287–2294 (2002)
8. Z.B. Zhou, P.W. Chen, F.L. Huang, Compressional punch loading test of a polymer bonded explosive simulant using digital image correlation method. J. Beijing Inst. Technol. **19**, 390–394 (2010)
9. M. Li, J. Zhang, C.Y. Xiong, Damage and fracture prediction of plastic-bonded explosive by digital image correlation processing. Opt. Lasers Eng. **43**, 856–868 (2005)
10. P.W. Chen, H.M. Xie, F.L. Huang, T. Huang, Y.S. Ding, Deformation and failure of polymer bonded explosives under diametric compression test. Polym. Test. **25**, 333–341 (2006)
11. S.J.P. Palmer, J.E. Field, J.M. Huntley, Deformation, strengths and strains to failure of polymer bonded explosives. Proc. R. Soc. **440**, 399–419 (1993)
12. D.G. Thompson, D.J. Idar, G.T. Gray III, Quasi-static and dynamic mechanical properties of new and virtually-aged PBX 9501 composites as a function of temperature and strain rate, in *Proceedings of the 12th International Detonation Symposium* (The Office of Naval Research, Arlington, VA, 2002), pp. 363–368
13. D.J. Idar, D.G. Thompson, G.T. Gray III, W.R. Blumenthal, C.M. Cady, P.D. Peterson, W.J. Wright, B.J. Jacquez, Influence of polymer molecular weight, temperature, and strain rate on the mechanical properties of PBX 9501. Shock Compress. Condens. Matter 821–824 (2001)
14. G.T. Gray III, D.J. Idar, W.R. Blumenthal, C.M. Cady, P.D. Peterson, High and low strain rate compression properties of several energetic material composites as a function of strain rate and temperature, in *Proceedings of the 11th International Detonation Symposium*, Snowmass Village, CO (1998), pp. 76–83
15. W.R. Blumenthal, G.T. Gray III, D.J. Idar, M.D. Holmes, P.D. Scott, C.M. Cady, D.D. Cannon, Influence of temperature and strain rate on the mechanical behavior of PBX 9502 and Kel-F 800TM, in *AIP Conference Proceedings*, Woodbury (New York, 2000), pp. 671–674
16. Y.C. Xiao, Y. Sun, Z.Q. Yang, L.C. Guo, Study of the dynamic mechanical behavior of PBX by Eshelby theory. Acta Mech. **228**, 1993–2003 (2017)
17. V. Sekkar, S. Gopalakrishnan, K.D. Ambika, Studies on allophanate–urethane networks based on hydroxyl terminated polybutadiene: effect of isocyanate type on the network characteristics. Eur. Polym. J. **39**, 1281–1290 (2003)

18. C.Y. Chen, X.F. Wang, L.L. Gao, Y.F. Zheng, Effect of HTPB with different molecular weights on curing kinetics of HTPB/TDI system. Chin. J. Energetic Mater. **21**, 771–776 (2013)
19. C.Y. Chen, X.F. Wang, H.T. Xu, X.J. Feng, L.L. Gao, H. Nan, Effects of temperature on curing stresses of casting plastic bonded explosives. Chin. J. Energetic Mater. **22**, 371–375 (2014)
20. X. Jin, K. Cai, W. Liu, Y.G. Dong, S.L. Hu, J.L. Yang, Effects of monomer content on internal stresses during solidification process and properties of green bodies by gelcasting. J. Chin. Ceram. Soc. **39**, 794–798 (2011)